

Eirik H. Herø<sup>\*1</sup>, Dr. Nicolas La Forgia<sup>1</sup>, Dr. Jannike Solsvik<sup>1</sup>, Prof. Hugo A. Jakobsen<sup>1</sup>

## Determination of Breakage Parameters in Turbulent Fluid-Fluid Breakage

### Abstract

Numerous sets of single particle breakage experiments are required in order to provide a sufficient database for improving the modeling of fluid particle breakage mechanisms. This work focuses on the interpretation of the physical breakage events captured on video. In order to extract the necessary information required for modeling the mechanisms of the fluid particle breakage events in turbulent flows, a well-defined image analysis procedure is necessary. Two breakage event definitions are considered; initial breakup and cascade breakup, and the reported breakage time, the number of daughter particles created and the daughter size distribution are significantly affected by the definition used. For each breakage event definition, an image analysis procedure is presented.

### Keywords

Droplet Breakage

Multiphase Flow

Image Analysis

Population Balance Equation

Turbulence

### Author Affiliation

<sup>1</sup>Department of Chemical Engineering, Norwegian University of Science and Technology (NTNU),  
Institutt for kjemisk prosessteknologi, NTNU, 7491 Trondheim, Norway

\* eirik.h.hero@ntnu.no

### 1. Introduction:

Several industries are interested in dispersed phase properties. In the oil and gas industry one of the challenges is separation of phases in a liquid-liquid system, e.g. oil in water. Many of the separators use gravity, buoyancy or other forces related to dispersed phase size, with larger drops separated faster than smaller drops. In the simulation of these systems, a framework able to predict the dispersed phase droplet size distribution is required. The population balance equation, PBE [1, 2], dynamically describes

the change of the dispersed phase particles as they are transported, coalescing and breaking. The present study focuses on breakage events in turbulent flow.

For an overview of the PBE and fluid particle breakage, the reader is referred to the supplementing information. In summary, the parameters needed from experimental investigations are mother drop size,  $D$ , breakage probability,  $P_b$ , breakage time,  $t_b$ , average number of daughters,  $\nu$ , and daughter size distribution function,  $P_D$ , as well as the continuous phase flow properties, in particular the turbulent kinetic energy dissipation rate,  $\varepsilon$ . Furthermore, it is important to know the fluid properties of both the dispersed phase, continuous phase and system properties, e.g. densities and interfacial tension.

The existing experimental work on the breakage event can be divided into macroscopic dispersed phase analysis, e.g. Coualoglou and Tavlarides [3], and single fluid particle analysis. Macroscopic investigations provide little information about local breakage functions [4], while the number of single fluid particle experiments is relatively scarce. Further complicating matters, many authors reporting fluid particle experiments provide no clear definition of the measured parameters, i.e. how the parameters are actually interpreted and measured in the experiments. Identifying the parameters, from a video or otherwise, is not a trivial task and different procedures give rise to deviating values. An overview is shown in Tab. 1, although the variation may be partly explained by the difference in experimental setup.

Several of the recent experimental investigations reported utilize high-speed imaging to capture the breakage event. Examples include Galinat et al. [5, 6], who conducted single oil drop breakage experiments in a channel with an orifice using 1.5-3 mm diameter n-heptane drops. Data on the droplets were extracted from video through commercial software, using the pixels in the contour of the droplets. The breakage probability, daughter size and daughter distribution were presented and correlated to the Weber number. Unfortunately, the different parameters determined were not specifically defined in the article.

Similarly, Andersson and Andersson [7] did not specify their definition of the breakage parameters when they studied a single oil drop, 1 mm dodecane or octanol, passing through a static mixer. Neither did they specify how they identified the measured breakage parameters from images. The turbulence energy dissipation rate was found by CFD, with a large eddy simulation, and experimentally, by particle

image velocimetry. The volume average dissipation rate, found to be 1.3-16.4  $\text{m}^2 \text{s}^{-3}$  depending on the continuous phase flow rate, was presented.

In the work of Maaß and coworkers, e.g. [8, 9, 10], single oil drops were investigated in a stirred tank and a channel with a single blade inducing turbulence, mimicking the flow around an impeller in a stirred tank. The videos were analyzed with commercial software [8] through an unknown procedure. The mother drops, toluene or petroleum, were reported from 0.54-3.1 mm. The breakup events were linked to the volume average turbulent energy dissipation rate of 0.3-1.8  $\text{m}^2 \text{s}^{-3}$  and the local maximum of 3.4-91.1  $\text{m}^2 \text{s}^{-3}$ . Maaß et al. [9] do indirectly define the parameters determined, stating that successive breakups are not considered. In addition, Maaß and Kraume [10] provided a decent attempt at statistical treatment of several breakage parameters. For the single blade setup, the breakage time was counted from the instant the drop passed the blade until the instance of fragmentation [10]. Nachtingall et al. [11] continued the work with an increased focus on statistical analysis. MATLAB was used to automatically extract the droplets projected area and perimeter and the shape and axes of drops were investigated. In addition, the breakage time was defined in two separate ways, the deformation and oscillation time. The deformation time is defined as starting with the last instance of a spherical mother drop and ending with the instance of fragmentation. In the oscillation time, the start is instead defined as the instance in which the mother drop passes the stirrer blade.

Solsvik and Jakobsen [12] investigated single fluid particle breakage in a stirred tank using several oils, i.e. Toluene, Petroleum, n-Dodecane and 1-Octanol, with sizes ranging from 0.6 to 4.0 mm. The videos were manually investigated for extraction of mother drop size, daughter numbers and breakage time. The breakup events were linked to the volume average dissipation rate, 1.14  $\text{m}^2 \text{s}^{-3}$ . Solsvik and Jakobsen [12] considered a breakup cascade to be a single event, thus the definition of the reported parameters deviate from that of Maaß and coworkers [8, 9, 10] and Nachtingall et al. [11].

From the literature, two clear definitions of the breakage event exist; initial breakup, e.g. Maaß et al. [9], and breakup cascade, as originally suggested by Solsvik et al. [13]. In the initial breakage definition, the event ends at the initial instantaneous breakup of the mother drop and the possible breakup cascade of the daughter drops are not considered. Thus the breakage time, daughter size and daughter number are only dependent on the first breakup. Conversely, in the breakup cascade, the breakup event can be a sequence of breakups. When deformed daughters undergo breakup, they are considered dependent on

the breakup of the initial mother drop. The definition adopted significantly affects the reported values for the breakage time, the daughter size distribution and the average number of daughters. Thus, the present work aims to outline an algorithm for the extraction of the breakage parameters from video.

## 2. Experimental setup

In order to investigate single droplet breakage an experimental facility has been constructed. A schematic can be seen in Fig. 1. The main part of the setup is a square channel, hereafter referred to as the breakage channel, which is 1 m long with a cross-section of 30 mm by 30 mm. It consists of two sides of glass and two sides of metal. The two glass sides allow the breakage event to be observed by two high speed cameras of the type Photron FASTCAM Mini AX100 540K M3 and illuminated by backlight. The two metal sides are equipped with transverse square rods to increase the turbulence generated at the wall, which in turn increase the general turbulence level in the channel. The rods are of size 3 mm by 3 mm and placed with a centerline distance of 10 mm. An example of a breakage event in one camera can be seen in Fig. 2, in which the rods on the channel walls are visible. The geometry allows for a flow pattern in the center of the channel with low shear and high turbulence intensity, which have been experimentally investigated and mapped by laser doppler velocimetry and presented in La Forgia et al.[13].

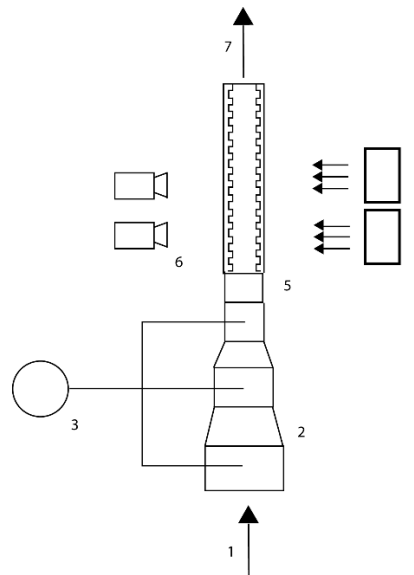


Figure 1: Schematic drawing of the experimental setup. 1. Water inlet, 2. Droplet generation section, 3. Oil syringe pump, 4. Illumination, 5. Breakage channel, 6. Two Cameras, 7. Water outlet.

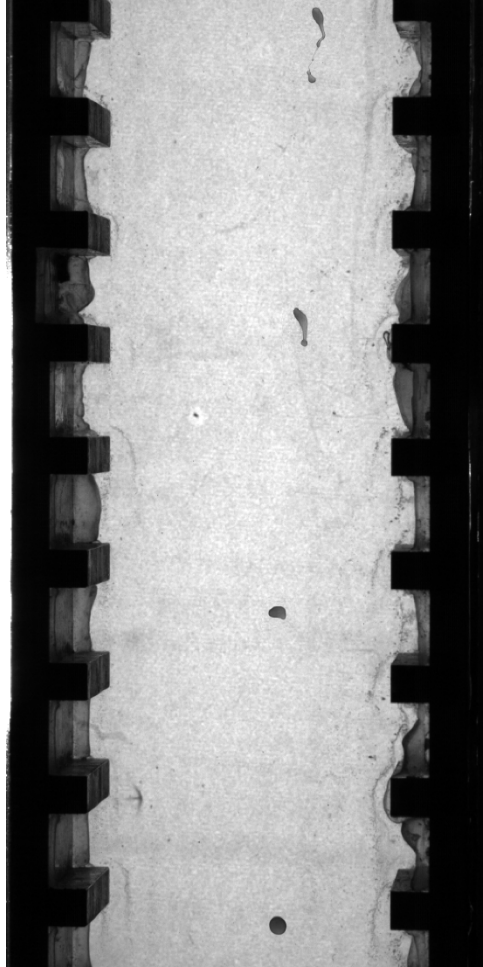


Figure 2: Collage of part of a breakup event observed by one camera.

Directly downstream of the breakage channel is a section for generating single oil droplets, hereafter referred to as the droplet generation section, which is similar to the setup used by Maaß and coworkers, e.g. [9]. The droplet generation section has three different regions, each with different cross-sectional areas. This allows for three different flow conditions for drop generation for each mean flow condition, i.e. turbulence level, in the breakage channel. For the creation of an oil droplet, a glass cylinder with a needle tip is inserted in one of the three regions. The size of the oil drop generated is determined by the size of the tip and the flow conditions of the section. Further, the glass cylinder is connected to a syringe pump with a 10 mL syringe.

Single 1-octanol drops are investigated with the algorithm proposed in the following section. The oil is dyed with black sudan, a non-water soluble dye, for increased contrast in the images, and the resulting properties can be seen in Tab. 2. The continuous phase is clean reverse-osmosis water at an area

average flowspeed of  $1.5 \text{ m s}^{-1}$ . The two cameras each have a resolution of  $1024 \times 1024$  and record at 4000 frames per second. Together they cover a region from 191 mm to 535 mm downstream of the inlet of the breakage channel, for a total length of 344 mm. The smallest drops detectable with this setup are about 0.17 mm, provided the contrast between the drop and continuous phase is large enough.

### 3. Image Analysis

The image analysis considers both of the breakup event definitions suggested in literature, i.e. the initial breakage definition and the cascade breakage definition. In order to compare the two definitions, each observed breakup event are interpreted through both the initial and the cascade breakage definition. Thus, the image analysis returns two separate sets of breakage parameters, one for each definition.

In order to establish the start of a breakage event, consider an initially stable drop. At this instance in time, it has a spherical shape. Then, the energy needed for breakup to occur is obtained, by e.g. collision with a turbulent eddy. The drop goes through a continuous deformation process and breaks into smaller drops stable at the new energy level. Thus, in either of the breakage event definitions, the start of the event is considered the instant of mother drop deformation, provided this deformation leads to a breakup. In the initial breakage definition, the event ends at initial breakup, i.e. the first instant of more than one drop. Possible successive breakups of the daughter drops are considered separate and independent breakage events. In the cascade breakage definition, on the other hand, the breakage event is considered finished at final breakup of intermediary daughters. In order for a daughter to be considered intermediary, it must undergo a continuous deformation, or in other terms, it must not obtain a spherical and stable shape. The difference of the two definitions is illustrated in Fig. 3. From the start instant of the breakage event, the continuous phase flow properties are found, while the size and number of daughter drops are found from the end instance. Further, the breakage time is the time between the two instants.

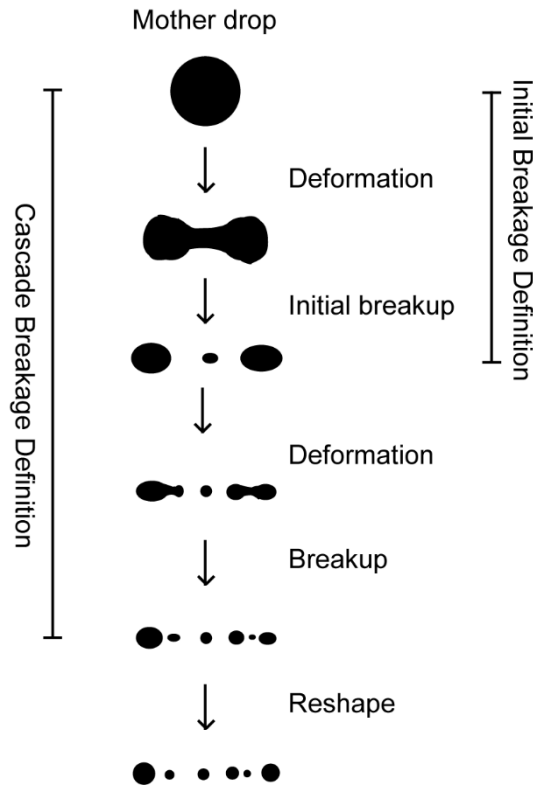


Figure 3: An illustration of the breakup cascade definition versus the initial breakup definition.

To extract the breakage parameters from two-dimensional video, the following algorithm is applied. Each frame is subtracted an image without a drop, i.e. the value of each pixel is subtracted the value of the corresponding pixel in an image with no drop. In the resulting image, each pixel without a drop present has a low grayscale value, while the pixels containing a drop have a higher greyscale value. Then, every pixel above a given greyscale value, dependent on light intensity in the video, is considered part of a drop. The procedure is illustrated in Fig. 4. Connected pixels are considered part of the same drop, and the area and position of the drops in the image are found from the pixels they occupy. In order to investigate the shape, the perimeter of the area is computed, as well as the minor axis and major axis of an ellipse with the same normalized second central moments as the area.

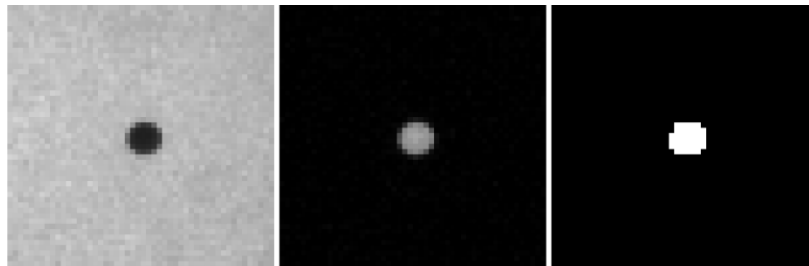


Figure 4: Image analysis; original grayscale image, subtracting background in grayscale and binary image.

The shape of the drop from the image is two-dimensional, while the real shape of the drops is three-dimensional. In order to determine the drop as stable or not stable, i.e. spherical or not spherical, the two-dimensional shape is first determined to be circular or not circular, as the projected area of a sphere is a circle. Two criteria are tested to identify circularity; first, the major and minor axes of the shape should be equal. Second, the actual perimeter of the drop shape is compared to the circumference of a circle with the same area as the drop. These two measures should be equal as well. If both the criteria are fulfilled, the drop is assumed circular in the plane. Yet, the drop may still be deformed in the third dimension and not spherical. However, as this deformation is unlikely to be stable in time, the drop is assumed spherical if it is found to be circular and it has the same area and perimeter for a few, e.g. 5, consecutive frames.

The start of the breakage event is taken to be the first frame in which the mother drop is deformed by a deformation that eventually leads to breakup. Thus, the start of the breakage event is a frame of a deformed, i.e. not spherical, drop who have been found to be circular for a number of the previous frames, e.g. 5. In the initial breakage definition, the breakage end is taken to be the first frame with more than one drop, i.e. the first frame with countable pixels between daughter drops, and further breakups are not considered. However, in the cascade breakage definition, the breakage end is the frame of the last intermediary daughter breakup. Daughter drops are considered intermediary if they are deformed, i.e. not considered spherical, between the breakup of the mother drop and the breakup of the daughter drop itself.

From the breakage start and breakage end instants, the breakage time is calculated from the number of frames in between and the framerate of the video. The number of daughters is the number of distinct drops at breakage end, i.e. the number of different regions of connected pixels. An example can be seen in Fig. 5, where the difference in breakage time,  $t_b$ , and number of daughter particles,  $\nu$ , due to breakage event definition is illustrated. Further, determining daughter sizes poses a significant challenge. A simplified and uncertain size determination is made from the ratio of the individual daughter's area to the total area of all daughter drops. E.g. if a daughter makes up half of the collective drop areas in the image, it is assumed to be half the size of the mother drop.



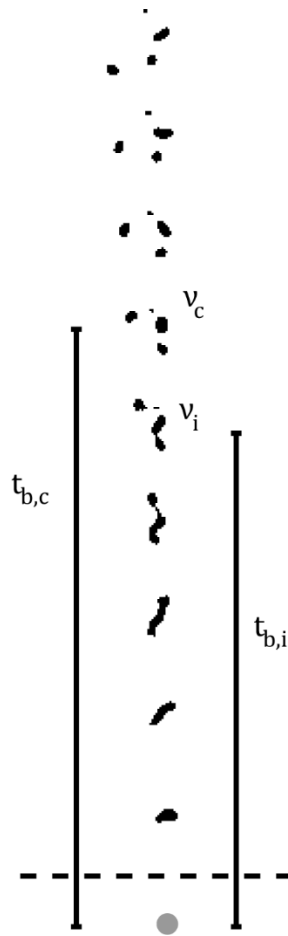


Figure 5: Output from image analysis and illustration of how the definition of the breakup event affects breakage time,  $t_b$ , and number of daughter particles,  $v$ . Cascade breakup is denoted by subscript  $c$  and initial breakup is denoted by subscript  $i$ .

The turbulent energy dissipation rate is found from the continuous phase average value at the position of the mother drop at breakage start. In the cases that the mother drop travels through large gradients in turbulence level, e.g. traveling close to the wall, the initial turbulent energy dissipation rate may not be representative. Thus, in such cases, a trajectory maximum value of the turbulent energy dissipation rate is also reported.

The breakage probability is determined from a set of experiments. The outcome of every single drop experiment is categorized as either a breakup event or no breakup event. After the whole series of experiments have been characterized in this way, the breakage probability is determined from the ratio of breakup events to the total number of drops observed.

#### 4. Results and Discussion

Although the use of high-speed cameras is common in the experimental work on droplet breakage reported in the literature, the interpretation of breakage parameters from the images is generally not provided or described in a vague manner. Sect. 3 outlines the framework used for extracting the breakage parameters from the video of the physical events in this work. In this section, the application of the image analysis to the current setup is discussed.

A single binary breakage event is shown in Fig. 6. Each image is a 50 pixels by 50 pixels region taken from the full image. First, a spherical mother drop undergoes a continuous deformation, starting at 0.25 ms, until separating after 37.5 ms. Then, the daughters obtain a spherical shape and the further development is not considered. In this special case, due to no daughters undergoing further breakage before becoming spherical, the cascade breakage definition coincide with the initial breakage definition and the breakage parameters obtained are the same. Breakage start is taken to be the start of deformation, i.e. 0.25 ms, and breakage end at separation, i.e. 37.5 ms, which gives a breakage time of 37.25 ms. From the breakage end image, the daughter number is found to be 2. Finally, the mother drop size is found from the time instance before deformation start, in which it was determined to be spherical. The daughter sizes are then found from their relative projected area of 62% and 38%, and taken to be 62% and 38% of the mother drop size.

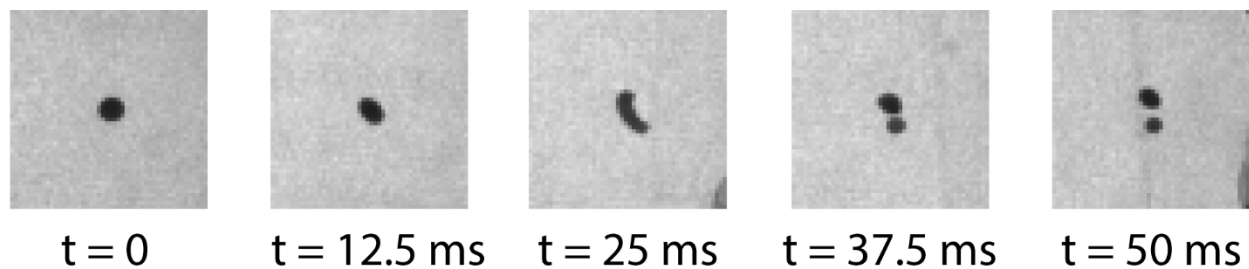


Figure 6: A sequence of images of an event leading to binary breakage.

Conversely, Fig. 7 shows an event of in which the breakage parameters of the two breakage definitions are significantly different. In order to highlight the determined information in each image, the binary image of the image algorithm is presented alongside. An originally spherical mother drop starts to deform at 0.25 ms. At 18 ms, the first separation into multiple drops is found and this time instance taken to be the end of the breakage event in the initial breakage definition. However, several of the

drops are still significantly deformed and found to break up until 28.25 ms. Thus, this time instance is taken to be the end of the breakage event in the cascade breakage definition. Further, in the initial breakage event definition, this event has a breakage time of 17.25 ms and 4 daughters. While in the cascade breakage event definition, this event has a breakage time of 28 ms and 9 daughters.

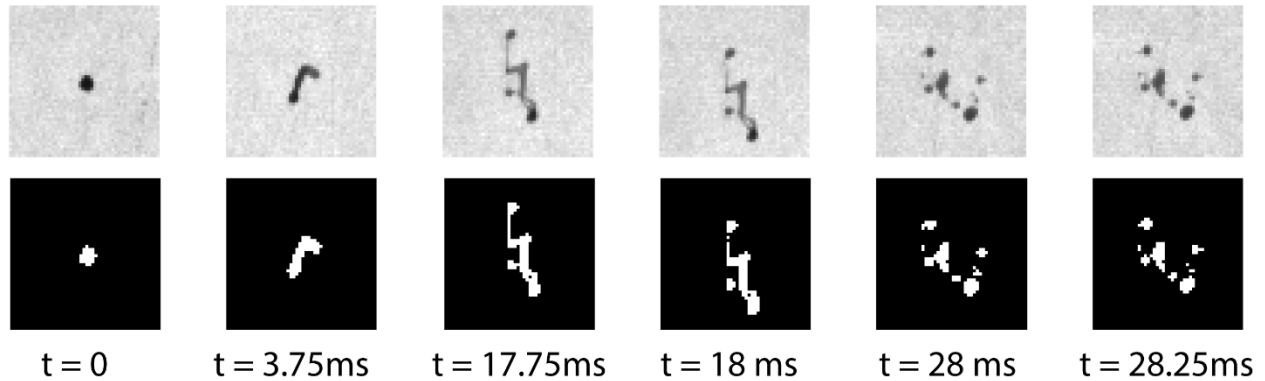


Figure 7: A sequence of images of an event leading to multiple breakage.

Ideally, the breakage events are checked for volume conservation. In order to do so, the daughter sizes must be determined exclusively from the information available after breakup. In one possible method, the daughters are assumed spherical and their projected area assumed circular. Then, from the projected area of the daughter, the diameter of an area equivalent circle is found, which is taken to be the size of the daughter. In the event that the daughter drops are observable at a stable and spherical shape, this method provides a better estimation of the daughter sizes compared with the method suggested in Sect. 3. However, in the initial breakage event definition the daughter drops may have a significantly deformed shape, as seen in Fig. 7. Additionally, the deformed daughter drops undergoing further breakage may not ever obtain a spherical shape. Thus, this method of determining daughter sizes is particularly challenging and may lead to significantly deviating values of volume conservation. On the other hand, in the cascade breakage event definition, the assumption that the daughters are spherical is more realistic. Furthermore, near spherical daughters may be identified from images after breakage end.

The resolution, both spatial and temporal, is an important factor determining the experimental uncertainty of the image analysis process. Firstly, at 4000 frames per second, there is a gap of 0.25 ms between each observation of the event. Subsequently, the instance of breakage start or breakage end may be determined to be almost 0.25 ms after the true value. Furthermore, the spatial resolution

represents a tradeoff; on one hand, it is beneficial to observe as much of the channel as possible to capture the whole cascade of all events. On the other hand, the two cameras have a set resolution of 1024 x 1024 pixels, which means that a certain zoom is required to capture the details of the breakage event. At low spatial resolution, detection and identification of the correct breakage end are further challenged, due to each pixel being considered either drop or not, e.g. two drops might be separated, but this is not detectable in the image. Furthermore, very small daughters of approximately 1 pixel in size may not be detectable continuously in subsequent images, due to changes in light intensity or due to the drop occupying only a small part of each pixel, in turn leading to a greyscale value below the threshold of detection.

Additionally, special care must be taken if the drop moves towards the wall. While the channel flow allows for a predictable turbulence level and low streamwise gradients in the turbulent energy dissipation rate in the center section of the channel, drops moving close to the wall experiences an increase in both shear and turbulence intensity. Thus, drops not broken before entering a region 1.5 mm from the rods on the wall are not considered to break from the turbulence alone, and while the events are recorded, they are not considered compatible with the events of drops broken outside of this region. In the particular event of a breakage in the center channel region, in which a possible intermediary daughter drop of the breakage cascade is transported into the wall region, no further breakage of the daughter drop is considered.

Further, special care is also taken for a deforming drop leaving the field of view of the cameras. In such cases the event is either considered finished or disregarded. If the drop leaving is a mother drop, it is considered to be an event with no breakage. On the other hand, if the drop is a possible intermediary daughter in the cascade breakage definition, the daughter is only considered finished breaking if it has been observed for at least 10 ms. If it has been observed less, the event is not considered for the cascade breakage, yet still counted in the initial breakage dataset.

Ideally, a program could interpret each event automatically. Unfortunately, daughter drops not detectable in continuous images, due to overlap or small size, makes automatic determination of the breakage cascade particularly challenging.

## 5. Conclusion

The image analysis of fluid particle breakage videos has been discussed. Specific definitions and physical interpretation of the breakage parameters are given, and the procedure for extracting the parameters from a series of images are elucidated.

The choice of breakage event definition, initial breakup or cascade breakup, is of significant importance to the reported values of breakup time, daughter distribution size and average number of daughters. While two definitions of the breakage event are considered in the literature, the experimental investigation should aim to provide the breakage parameters of both definitions. The accuracy of the experimental data is dependent on being extracted from the correct definition of the breakage event, and as such, both sets of data are relevant until one of the definitions of the breakage event can be reconciled with the physical breakage phenomena.

The determination of daughter sizes are a particular challenge. In the initial breakage event definition, the available information of each drop obtainable from two-dimensional imaging is limited. Thus, coarse assumptions must be made. Conversely, while the cascade breakage event definition is challenging to implement automatically, it does have the advantage of observing each daughter drop in a stable state, allowing volume conservation verification.

## 6. Acknowledgment

This work was carried out as a part of SUBPRO, a Research-based Innovation Centre within Subsea Production and Processing. The authors gratefully acknowledge the financial support from SUBPRO, which is financed by the Research Council of Norway, major industry partners and NTNU.

### Symbols used

#### Symbols

$D$	[m]	Droplet diameter
$P_b$	[-]	Breakage probability
$P_D$	[m <sup>-1</sup> ]	Daughter size distribution function
$t_b$	[s]	Breakage time

#### Greek letters

$\varepsilon$	[m <sup>2</sup> s <sup>-3</sup> ]	Turbulent kinetic energy dissipation rate
---------------	-----------------------------------	---

$\mu$	[mPa s]	Dynamic viscosity
$\nu$	[-]	Average number of daughters
$\rho$	[kg m <sup>-3</sup> ]	Density
$\sigma_i$	[mN m <sup>-1</sup> ]	Interfacial Tension

## References

- [1] D. Ramkrishna, *Population Balance: Theory and Applications to Particulate Systems in Engineering*, Academic Press, San Diego **2000**
- [2] H.A. Jakobsen, *Chemical Reactor modeling*, 1st ed., Springer-Verlag, Berlin **2008**.
- [3] C.A. Coulaloglou, L.L. Tavlarides. *Chem. Eng. Sci.* **1977**, *32(11)*, 1289 – 1297. DOI: 10.1016/0009-2509(77)85023-9
- [4] J. Solsvik, S. Tangen, H.A. Jakobsen, *Rev. Chem. Eng.* **2013**, *29(5)*, 241–356. DOI: 10.1515/revce-2013-0009
- [5] S. Galinat, O. Masbernat, P. Guiraud, C. Dalmazzone, C. Noik, *Chem. Eng. Sci.* **2005**, *60(23)*, 6511-6528. DOI: 10.1016/j.ces.2005.05.012
- [6] S. Galinat, L. Garrido Torres, O. Masbernat, P. Guiraud, F. Risso, C. Dalmazzone, C. Noik, *AIChE J.*
- [7] R. Andersson, B. Andersson, *AIChE. J.* **2006**, *52*, 2020-2030. DOI: 10.1002/aic.10831
- [8] S. Maaß, A. Gäbler, A. Zaccone, A.R. Paschedag, M. Kraume. *Chem. Eng. Res. Des.* **2007**, *85(5)*, 703-709. DOI: 10.1205/cherd06187
- [9] S. Maaß, S. Buscher, S. Hermann, M. Kraume, *Biotechnol. J.* **2011**, *6*, 979–992. DOI: 10.1002/biot.201100161
- [10] S. Maaß, M. Kraume, *Chem. Eng. Sci.* **2012**, *70*, 146-164. DOI: 10.1016/j.ces.2011.08.027.
- [11] S. Nachtigall, D. Zedel, M. Kraume, *Chin. J. Chem. Eng.* **2016**, *24*, 264–277. DOI: 10.1016/j.cjche.2015.06.003
- [12] J. Solsvik, H.A. Jakobsen, *Chem. Eng. Sci.*, **2015**, *131*, 219-234. DOI: 10.1016/j.ces.2015.03.059 **2006**, *53*: 56-68. DOI: 10.1002/aic.11055
- [13] J. Solsvik, S. Maaß, H.A. Jakobsen, *Ind. Eng. Chem. Res.*, **2016**, *55 (10)*, 2872–2882 DOI: 10.1021/acs.iecr.6b00591
- [14] N. La Forgia, E.H. Herø, J. Solsvik, H.A. Jakobsen. *Chem. Eng. Sci.* **2019**, *195*, 159-178. DOI: 10.1016/j.ces.2018.11.039

Tables with Headings:

Reference	Experimental Setup	Breakage Definition	Average Number of Daughter Drops	Breakage time [ms]
Galinat et al. [5, 6]	Orifice Pipe Flow	Unknown	2-11.5	45-65
Andersson and Andersson [7]	Static Mixer	Unknown	2-9	4-11
Maass et al. [9, 10]	Mimic Stirred Tank	Initial Breakup	2-2.4	12-35
Solsvik and Jakobsen [12]	Stirred tank	Breakup Cascade	2-9+	5-160

Table 1: Selected single drop experiments in literature.

	Density $\rho$ [ $\text{kg m}^{-3}$ ]	Interfacial Tension $\sigma_i$ [ $\text{mN m}^{-1}$ ]	Dynamic viscosity $\mu$ [ $\text{mPa s}$ ]
1-Octanol	825	8.20	9.09

Table 2: Properties of 1-Octanol dyed with black sudan.